radation of these anesthetics in in vitro and in vivo experiments. Whether individual enantiomers of I, II, and III may have clinical advantages with respect to potency, toxicity, times of onset of action or recovery, or olfactory properties remains to be seen. While we have developed efficient syntheses of each of the enantiomers of halothane and enflurane (*13*), the remaining problems associated with carrying out the necessary in vivo studies, including the task of preparing sufficiently large quantities of each pure isomer, are not trivial. Nevertheless, it is important to establish whether any clinical advantage may be gained by the use of one particular stereoisomer of these anesthetics. This question is of particular interest in view of the increasing awareness of the potential significance of drug chirality within the chemical, medical, and governmental regulatory communities (*14*).

REFERENCES AND NOTES

1. R. K. Calverley, *Clinical Anesthesia* (Lippincott, Philadelphia, 1989), pp. 3–32.
2. _____, *Surv. Anesth.* **29**, 170 (1986).
3. C. W. Suckling, *Br. J. Anesth.* **29**, 466 (1957).
4. R. C. Terrell, L. Speers, A. J. Szur, J. Treadwell, T. R. Ucciardi, *J. Med. Chem.* **14**, 517 (1971).
5. W. C. Stevens and H. G. G. Kingston, *Clinical Anesthesia* (Lippincott, Philadelphia, 1989), pp. 293–323.
6. A. R. Dluzewski, M. J. Halsey, A. C. Simmonds, *Mol. Aspects Med.* **6**, 459 (1983).
7. N. P. Franks and W. R. Lieb, *Nature* **310**, 599 (1984).
8. A. S. Evers, B. A. Berkowitz, D. A. d'Avignon, *ibid.* **328**, 157 (1987).
9. J. J. Kendig, J. R. Trudell, E. N. Cohen, *Anesthesiology* **39**, 518 (1973).
10. Capillary columns with per-*n*-pentylated α-cyclodextrin (Lipodex A) are available from Macherey-Nagel (Dueren, Germany).
11. W. A. König, S. Lutz, G. Wenz, *Angew. Chem.* **100**, 989 (1988); *Angew. Chem. Int. Ed. Engl.* **27**, 979 (1988).
12. W. A. König, D. Icheln, T. Runge, I. Pforr, A. Krebs, *J. High Res. Chromatogr.* **13**, 702 (1990).
13. D. L. Pearson, thesis, Cornell University, Ithaca, NY (1990).
14. W. H. De Camp, *Chirality* **1**, 2 (1989); S. Borman, *Chem. Eng. News* **68** (no. 28), 9 (1990).
15. J. Bouche and M. Verzele, *J. Gas Chromatogr.* **6**, 501 (1968).
16. W. A. König and K. Ernst, *J. Chromatogr.* **280**, 135 (1983).

17. Partial support of this work was provided in its early stages by NIH grant no. GM37018. We are indebted to G. Vernice and the Anaquest Corporation for subsequent support and encouragement. This paper was completed while J. M. was a fellow at the Center for Advanced Study in the Behavioral Sciences, partially supported by NSF grant BNS-8700864.

13 August 1990; accepted 15 November 1990

Regulation of the Apolipoprotein AI Gene by ARP-1, a Novel Member of the Steroid Receptor Superfamily

JOHN A. A. LADIAS AND SOTIRIOS K. KARATHANASIS

Apolipoprotein AI (apoAI) is a lipid-binding protein that participates in the transport of cholesterol and other lipids in the plasma. A complementary DNA clone for a protein that bound to regulatory elements of the apoAI gene was isolated. This protein, designated apoAI regulatory protein–1 (ARP-1), is a novel member of the steroid hormone receptor superfamily. ARP-1 bound to DNA as a dimer, and its dimerization domain was localized to the COOH-terminal region. ARP-1 also bound to a thyroid hormone–responsive element and to regulatory regions of the apoB, apoCIII, insulin, and ovalbumin genes. In cotransfection experiments, ARP-1 down-regulated the apoAI gene. The involvement of ARP-1 in the regulation of apoAI gene expression suggests that it may participate in lipid metabolism and cholesterol homeostasis.

CHOLESTEROL HOMEOSTASIS IS ACcomplished by the integration of pathways that govern cellular biosynthesis, uptake, and excretion of cholesterol (*1*). The high-density lipoproteins (HDL) and their major protein constituent, apoAI, participate in the excretion process (*1*). High-density lipoprotein removes cholesterol from peripheral tissues and transports it, either directly or via other plasma lipoproteins, to the liver, where it is excreted. It is thought that, because of their involvement in cholesterol excretion, apoAI and HDL are important in protection against coronary heart disease (*2*). Indeed, genetic deficiencies in apoAI and HDL are associated with excessive intracellular cholesterol accumulation and premature atherosclerosis (*2*).

The apoAI gene is expressed primarily in liver and intestine (*3*) and is regulated by diet (*4, 5*), estrogen (*5, 6*), thyroid hormone (*7*), and temporal factors during development (*3, 5*). The −222 to −110 DNA region upstream of the human apoAI gene functions as a liver-specific transcriptional enhancer (*8*). To identify the factors that regulate the apoAI enhancer in liver cells, we used a DNA fragment from the apoAI gene that included the region between −256 to −80 bp upstream of the transcription initiation site as a probe in deoxyribonuclease I (DNase I) protection experiments. Nuclear extracts from rat liver contained proteins that bound to four sites: A (−222 to −193), B (−169 to −149), C (−135 to −118), and D (−114 to −108, corresponding to the CCAAT homology) (Fig. 1). In contrast, extracts from tissues and cells that do not express apoAI (rat spleen, kidney, brain, and HeLa), protected only site A (Fig. 1) (*9*). Mutagenesis of sites A, B, or C indicate that protein binding to all three sites is essential for maximal expression of apoAI in human hepatoma (HepG2) cells (*8*).

To characterize the proteins that bound to site A, an oligonucleotide that corresponded to the A site (oligo A) was used as a probe to screen several λgt11 cDNA expression libraries (*10*). One positive clone (λHP-1) was isolated from a human placenta library, and binding-specificity spot tests (*10*) showed that the fusion protein produced by λHP-1–infected bacteria bound specifically to oligo A. The sequence of the insert was determined and its reading frame was established (Fig. 2A). The sequence of a clone that contained additional 5′ sequences (λHP-16) (*10*) revealed an upstream in-frame termination codon (underlined in Fig. 2A), thus placing the initiator methionine at position 343/345 and predicting a 414–amino acid protein, which we named apoAI regulatory protein–1 (ARP-1).

Comparison of ARP-1 with proteins in the GenBank database (*10*) revealed a similarity to human Ear-3 and Ear-2 "orphan" steroid hormone receptors (*11*) and the *Drosophila* Seven-up proteins (types 1 and 2), which regulate retinal cell differentiation (*12*). A cysteine-rich region of ARP-1 that corresponds to the DNA binding domain of the steroid hormone receptors (amino acids 79 to 144) (Fig. 2A), shares 98.5, 89.4, and 92.4% identity with the Ear-3, Ear-2, and Seven-up, respectively. The ARP-1 COOH-terminal domain (amino acids 145 to 414) is 95, 67, and 84.4% similar to Ear-3, Ear-2, and Seven-up (type 1), respectively, whereas the NH_2-terminal domain (amino acids 1 to 78) shows limited similarity. Thus, it appears that these proteins belong to an ancestral subfamily of nuclear receptors, which we refer to as the ARP subfamily (*13*). The high degree of evolutionary conservation of this subfamily suggests functional conservation and implies regulation of its members by similar ligands. The Ear-3 gene has been localized to human chromosome 5 (*11*), whereas ARP-1 is on chromosome 15 (*9*),

Laboratory of Molecular and Cellular Cardiology, Department of Cardiology, Children's Hospital, and Department of Cellular and Molecular Physiology, Harvard Medical School, Boston, MA 02115.

indicating that these proteins are encoded by two distinct genes. Northern (RNA) blot analysis, with the use of an ARP-1 specific probe (3′-ARP gene probe, see legend to Fig. 2), revealed a single ~4.5-kb transcript in all human tissues and cell types examined (Fig. 2B), thus explaining, at least in part, the ubiquitous tissue distribution of nuclear proteins that bound to site A (Fig. 1).

Translation in vitro of RNA derived from the insert of λHP-1 produced a protein of ~47 kD. Gel retardation analysis showed that in vitro translated ARP-1 bound specifically to oligo A, forming a complex similar in mobility to that of HeLa nuclear proteins (Fig. 3A). However, oligo C (a DNA probe that contained site C) competed with formation of this complex (Fig. 3A, lane 5). Methylation interference analysis demonstrated that the purine residues of oligo A that were contacted by in vitro translated ARP-1 were identical to those contacted by rat liver and HeLa nuclear proteins (Fig. 3B). Furthermore, ARP-1 produced in COS-1 cells protected site A from DNase I cleavage (Fig. 3C). These results indicate that the DNA binding specificity of ARP-1 is identical to that of nuclear proteins that bind to site A. Although ARP-1 bound to oligo C (Fig. 3A, lane 5 and Fig. 3D), it did not protect site C from DNase I (Fig. 3C, lane 1), suggesting that sequences surrounding this site may influence its interaction with ARP-1.

To determine whether ARP-1 can interact with cis-acting elements of other genes, in vitro–translated protein was tested for binding to several oligonucleotides (Table 1). ARP-1 bound with high affinity and specificity to COUP, APOCIII, APOB, INS, and TRE (thyroid hormone–responsive element), poorly to ERE (estrogen responsive element) and LF-B2, and not at all to HNF-4 and LF-A1 (Fig. 3D). Binding to COUP and INS was not unexpected because the transcription factor that binds to these elements, is Ear-3 (*14*), whose DNA binding domain is almost identical to that of ARP-1. In fact, Ear-3 also bound to elements recognized by ARP-1 (*9*), which suggests that both proteins may be involved in the regulation of apoAI, apoCIII, apoB, insulin, and ovalbumin genes.

A consensus sequence of the ARP-1 DNA binding site is composed of two directly repeated octanucleotides (Table 1) and differs from various hormone responsive elements, which are generally palindromic repeats (*15*). However, ARP-1 also recognized the palindromic TRE. The property of ARP-1 to discriminate between TRE and ERE in combination with the ability of the thyroid hormone receptor to bind to both with opposite transcriptional effects (*16*) may have significant implications for the regulation of genetic networks responsive to thyroid hormone.

The DNA binding domain of ARP-1 was determined by testing several ARP-1 deletion mutants (Fig. 4, A and B) for binding to site A. Deletion of amino acid residues 2 to 77 in mutant ΔA1 did not affect binding (Fig. 4C, lane 2). In contrast, deletion of 78,

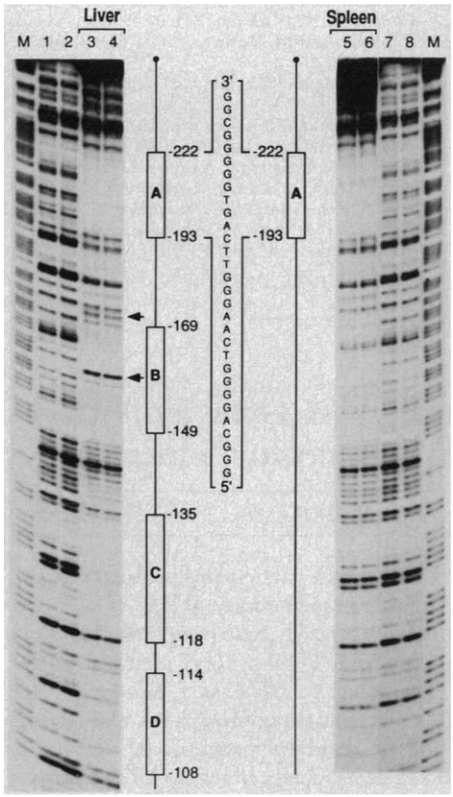

Fig. 1. DNase I protection of the −256 to −80 apoAI DNA region (noncoding strand) in the presence of rat liver (lanes 3 and 4), rat spleen (lanes 5 and 6), and in the absence of nuclear extracts (lanes 1, 2, 7, and 8). Lanes M: Maxam-Gilbert G + A reaction (*10*). Protected regions are indicated by boxes, and their approximate borders are numbered according to the transcription start site. Liver extract–induced DNase I hypersensitive sites are indicated by arrows. The sequence of site A (noncoding strand) is shown in brackets. Nuclear extracts were prepared as described (*22*). A DNA fragment (~1 to 2 fmol), containing the −256 to −80 human apoAI region 5′-^{32}P-labeled at the noncoding strand, was incubated on ice with 40 μg (lanes 3 and 5) or 70 μg (lanes 4 and 6) of nuclear protein in the presence of 50 mM KCl, 10 mM Hepes, pH 7.8, 10% glycerol, 0.1 mM EDTA, 0.5 mM phenylmethylsulfonyl fluoride (PMSF) and 0.5 mM dithiothreitol (DTT) (buffer A), 2% polyvinyl alcohol, 9 mM $MgCl_2$, 2.5 mM $CaCl_2$, and 1 μg of poly(dI-dC). The digestion was carried by 50 ng of DNase I (Worthington) at 20°C for 60 s and stopped by addition of five volumes of 100 mM tris-HCl, pH 8, 100 mM NaCl, 1% SDS, 10 mM EDTA, 100 μg of proteinase K, and incubated at 65°C for 15 min. DNase I (5 ng) was used when no extract was present. Nucleic acids were extracted with a mixture of phenol, chloroform, isoamyl alcohol (25:24:1), precipitated with ethanol, and analyzed on a 6% polyacrylamide–8 M urea sequencing gel.

Table 1. Oligonucleotides tested for ARP-1 binding. All oligomers had a 5′ GATC overhang. Spaces were introduced in the sequences for best alignment. A region of maximal similarity among oligos that bound ARP-1 (bold) was used to generate a consensus. Each nucleotide in the consensus is present in >50% of the aligned sequences. N represents any nucleotide or absence of such. Direct repeats are underlined.

Oligo	Gene of origin	Position	Reference	Sequence	Binding
A	Human apoAI	−214/−192	(*20*)	ACTGAACCCTTGACCCCTGCCCT	+
C	Human apoAI	−136/−114	(*20*)	GCTGA–TCCTTGAACTCTTAAGTT	+
APOCIII	Human apoCIII	−86/−70	(*25*)	GGAGGTGA–CCTTTG—CCCA	+
APOB	Human apoB	−80/−60	(*26*)	GGCGC–CCTTTGGACCTTTTGC	+
COUP	Chicken ovalbumin	−91/−64	(*14*)	TCAGAAGTTTGA–CCTTTGACACCATAGA	+
INS	Rat insulin II	−63/−36	(*27*)	AAGCACCCCCCCCCTGA–CCCCTG–GACTT	+
TRE	Artificial palindrome		(*16*)	TCAGGTCATGACCTGA	+
Consensus				TGANCCCTTGACCCCT	
AMUT1	Human apoAI	−214/−192	(*8*)	ACTGAACCCGGGACCCCTGCCCT	−
ERE	*Xenopus* vitellogenin A2	−335/−315	(*28*)	CATCAGGTCACTGTGACCTGACG	−/+
LF-B2	Human α1-antitrypsin	−91/−70	(*29*)	TAACTGGGGTGA—CCTTGGTTAA	−/+
HNF-4	Mouse transthyretin	−151/−130	(*30*)	CTACACAAATATGA–ACCTTG–CC	−
LF-A1	Human α1-antitrypsin	−128/−99	(*29*)	CCAGCCAGTGGA—CTTAGCCCCTGTTTGCTC	−

107, 179, or 215 residues at the COOH-terminal domain in mutants ΔA2, ΔA3, ΔA4, and ΔA5, respectively, eliminated binding (Fig. 4C, lanes 3 to 6); deletion of 244 residues in ΔA6 restored DNA binding (Fig. 4C, lane 7). Moreover, deletion of both NH_2- and COOH-terminal domains in ΔA7 did not affect binding (Fig. 4C, lane 8), thus mapping the DNA binding domain between residues 78 and 170. These results indicate that, in the absence of the 337–414 region, DNA binding is inhibited by sequences COOH to residue 170, and at least a portion of these sequences is located in the 171 to 199 region.

To determine whether ARP-1 binds to DNA as dimer, we cotranslated equal amounts of ARP-1 and ΔA1 mRNA in vitro, and the products were tested for binding to site A in gel retardation assays. In addition to complexes that corresponded to ARP-1 and ΔA1 alone, complexes with intermediate mobility (heterodimers) were also formed (Fig. 4C, lane 9), indicating that one molecule each of ARP-1 and ΔA1 bound concomitantly to site A. Heterodimers were also formed when the two proteins were translated separately, mixed, and used in gel retardation assays (Fig. 4C, lane 10). These results indicate that ARP-1 binds to DNA as a dimer, the NH_2-terminal domain is not required for dimer formation, and dimerization can occur after translation. In contrast, heterodimers were not observed with any of the COOH-terminal deletion mutants (Fig. 4C, lanes 11 and 12), indicating that sequences within the COOH-terminal domain are required for formation of dimers that are capable of DNA binding, and that at least a portion of these sequences is located in the 337 to 414 region. Because mutants ΔA6 and ΔA7 lacked the COOH-terminal domain, they may have bound to DNA as monomers (Fig. 4C, lanes 7, 8, and 12). Indeed, heterodimers were not observed when ΔA6 and ΔA7 were cotranslated (Fig. 4C, lane 13). Thus, unlike the estrogen receptor (*17*), ARP-1 does not seem to contain a dimerization domain within its DNA binding region. The COOH-terminal domain of ARP-1 contains several hydrophobic heptad repeats, indicating its potential for coiled-coil interactions. Specifically, a heptad repeat in the region 357–391 is highly conserved among several steroid receptors and the analogous region of the estrogen receptor is required for dimerization and high-affinity DNA binding (*18*).

Additional gel retardation experiments showed that over a wide range of concentrations, ARP-1 formed only one complex with oligo A (complex III, Fig. 4D, lanes 1 to 5). The curve of complex III formation

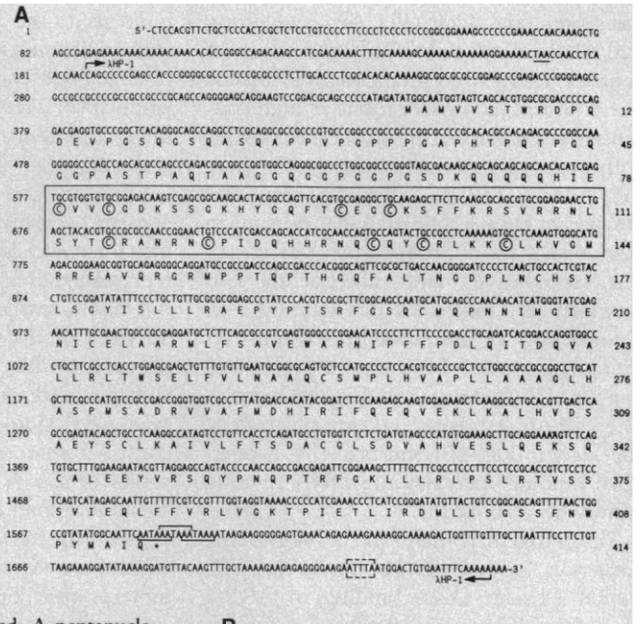

Fig. 2. (**A**) Nucleotide and derived amino acid sequence of the ARP-1 cDNA clone λHP-16. Numbers on the left and right indicate nucleotide and amino acid residues, respectively. Abbreviations for the amino acids are A, Ala; C, Cys; D, Asp; E, Glu; F, Phe; G, Gly; H, His; I, Ile; K, Lys; L, Leu; M, Met; N, Asn; P, Pro; Q, Gln; R, Arg; S, Ser; T, Thr; V, Val; W, Trp; and Y, Tyr. The λHP-1 insert is shown between arrows. A termination codon upstream of the initiator ATG is underlined. A 66–amino acid region that corresponds to the DNA binding domain of the steroid receptors is boxed and cysteines implicated in formation of Zn fingers are circled. Three overlapping consensus polyadenylation signals are bracketed. A pentanucleotide (ATTTA) implicated in regulation of mRNA stability (*23*) is enclosed in a dashed box. (**B**) ARP-1 hybridization patterns in total RNA (20 μg) from the indicated human fetal tissues and the cell lines: HepG2 and Hep3B (hepatoma), Caco-2 (intestinal carcinoma), HeLa (epitheloid carcinoma), HUSK-1 (skeletal myoblasts), and K562 (myelogenous leukemia). ARP-1 mRNA is detected in fetal thymus with a longer exposure. The 18*S* and 28*S* ribosomal RNA sizes are indicated. RNA was isolated, separated by electrophoresis, blotted onto nitrocellulose filters, and hybridized (*24*) with the 3′-ARP gene probe, a ~2.2-kb genomic DNA fragment spanning 433 nucleotides at the 3′ of λHP-1 and extending to 3′ direction.

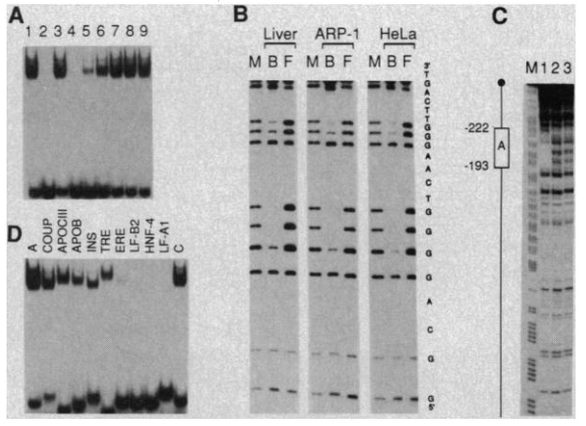

Fig. 3. (**A**) DNA binding specificity of ARP-1 assayed by gel retardation. The λHP-1 insert was subcloned in the Eco RI site of pGEM-4 (pGEM–ARP-1A), linearized with Xba I, transcribed in vitro by SP6 RNA polymerase, and the resulting RNA was translated in a rabbit reticulocyte lysate system (Promega) in the presence of [^{35}S]methionine, as recommended by the manufacturer. For gel retardation, proteins were incubated with ^{32}P-labeled oligo A (10 fmol) for 30 min on ice in the presence of 10 mM tris-HCl, pH 7.5, 50 mM NaCl, 5% glycerol, 1 mM EDTA, 1 mM DTT, and either 3 μg (for nuclear extracts) or 0.25 μg (for in vitro translated proteins) of poly (dI-dC), and separated by electrophoresis in nondenaturing gels. Two films were placed against the dried gel but only the film exposed to ^{32}P radiation is shown. Lane 1, HeLa nuclear proteins (5 μg); lane 2, unprogrammed reticulocyte lysate (2 μl); and lanes 3 to 9, in vitro translated ARP-1. Complexes were competed with 50-fold molar excess of unlabeled oligo A (lane 4), several double-stranded oligomers spanning the apoAI regions −136 to −114 (oligo C, lane 5), −177 to −148 (lane 7), and −116 to −84 (lane 8), an unrelated oligomer (lane 9), and oligo AMUT1 (lane 6). (**B**) Methylation interference analysis of in vitro translated ARP-1, rat liver, and HeLa nuclear extracts with an oligo A probe. The noncoding strand of oligo A was 5′-^{32}P-labeled, annealed with ~0.1-fold molar excess of its unlabeled complementary strand, partially methylated with dimethyl sulfate and used for preparative gel retardation. Protein-bound and free probe were recovered by electroelution onto NA-45 DEAE membrane (S & S), incubated in 10 mM sodium phosphate–1 mM EDTA (pH 8.0) at 90°C for 15 min, and then cleaved with 0.1 M NaOH at 90°C for 30 min. The samples were precipitated with ethanol and analyzed on a 20% polyacrylamide–8 M urea gel. Lanes B, protein-bound probe; F, free probe; and M, G + A sequencing ladder. Contact points are denoted by asterisks. (**C**) DNase I protection of the −256 to −80 apoAI fragment with whole-cell extracts (10 μg) from COS-1 transfected with pMA (lane 1) or pMB (lane 2) (*21*). Lane 3, absence of extracts. Lane M, G + A ladder. (**D**) Binding of in vitro translated ARP-1 to the indicated oligos (see also Table 1), assayed by gel retardation.

has a sigmoidal shape (Fig. 4E), suggesting that ARP-1 binds to DNA cooperatively. In contrast, at low concentrations, ΔA6 formed one complex (complex I), but at high concentrations it formed an additional complex with reduced mobility (complex II) (Fig. 4D, lanes 6 to 10). Thus, it seems that absence of the COOH-terminal domain in ΔA6 results in noncooperative binding of one (complex I) and subsequently two (complex II) molecules per binding site. Comparison of the protein amounts required to convert 50% of the probe into complex III (0.75 μg, Fig. 4E) and complex II (~50 μg, estimated by extrapolation of the curve in Fig. 4F), indicates that cooperative binding increases the DNA binding affinity by ~70 fold.

Taken together, these results suggest that sequences located COOH to residue 170 inhibit efficient DNA binding of ARP-1 monomers. The precise mechanism for this inhibition is not clear, but it is possible that the DNA binding domain is masked by a region in the COOH-terminal domain, either directly or by interacting with another protein as in the case of the glucocorticoid receptor and hsp 90 (*19*). Dimerization of ARP-1, an event that requires the 337–414 region, results in presentation (unmasking) of the DNA binding domain and efficient binding to DNA.

To study the effect of ARP-1 on apoAI gene expression, we cotransfected reporter plasmids that contained the bacterial chloramphenicol acetyl transferase (CAT) gene under the control of the apoAI promoter and enhancer (−256AI.CAT and −192AI.CAT) (*20*) and increasing amounts of a construct expressing ARP-1 (pMA) (*21*) into HepG2 cells. Overexpression of ARP-1 repressed the expression of −256AI.CAT, but had a smaller effect on −192AI.CAT activity (Fig. 5), suggesting that the repression was mediated primarily through site A and to a lesser extent through site C. However, ARP-1 did not affect the activity of a construct that contained one or multiple copies of site A in front of the thymidine kinase promoter (*9*), suggesting that ARP-1 does not function as a direct repressor but its effects on transcription may depend on promoter context. Furthermore, preliminary experiments showed that both ARP-1 and Ear-3 down-regulated the apoAI and apoCIII genes in HepG2 cells (*9*).

Previous studies have shown that binding of positive regulators to site A is essential for maximal levels of apoAI expression in HepG2 cells (*8, 20*). Indeed, two more nuclear receptors have been identified that bind to site A and activate transcription (*9*), indicating that this site is responsive to both positive and negative regulatory proteins.

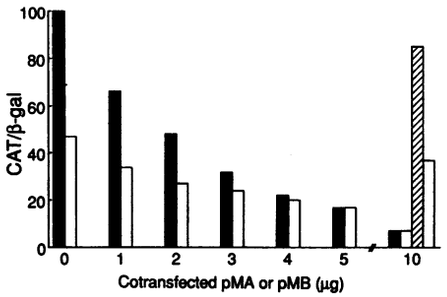

Fig. 5. Repression of the apoAI enhancer activity by ARP-1. The reporter plasmids −256AI.CAT and −192AI.CAT (*20*) (15 μg each), were cotransfected with pRSV–β-gal (3 μg) and the indicated amounts of pMA or pMB constructs (*21*) in HepG2 cells, as described (*20*). CAT assays were performed 48 hours after transfection, and the obtained values were normalized to β-galactosidase (β-gal) activities, as described (*20*). The average values (CAT/β-gal) of at least three independent experiments are shown as the percentages of the average value obtained with cells transfected with −256AI.CAT alone. Black bars, −256AI.CAT + pMA; white bars, −192AI.CAT + pMA; hatched bars, −256AI.CAT + pMB; stippled bars, −192AI.CAT + pMB.

The interplay of these factors could result in induction or repression of the apoAI gene in response to various signals. In this context, high amounts of dietary fat and cholesterol reduce significantly hepatic apoAI mRNA (*4*), raising the possibility that ARP-1 and Ear-3 may participate in mediating such effects. In the absence of information about ligand regulation of these proteins, their physiological function remains to be defined. Nevertheless, the observation that these regulators could influence apolipoprotein concentrations suggests that they may be an important part of the signal transduction mechanisms contributing to cholesterol homeostasis.

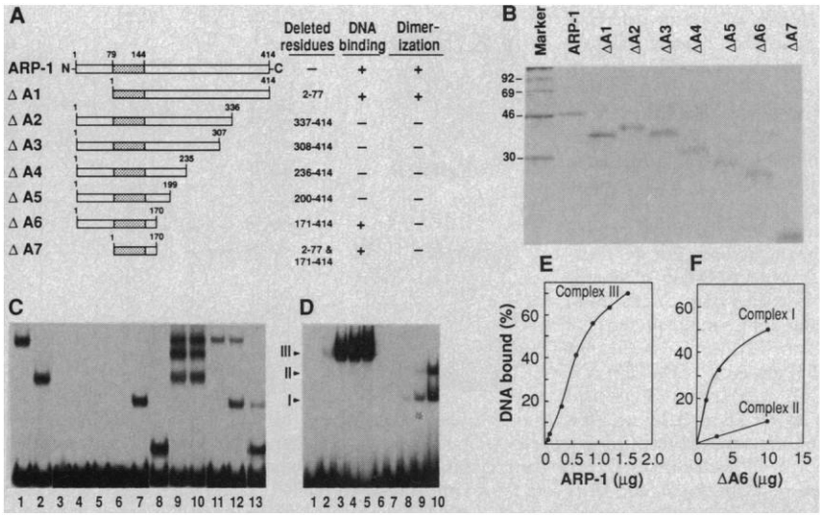

Fig. 4. (**A**) Schematic representation, DNA binding, and dimerization properties of ARP-1 and its deletion mutants (*21*). The DNA binding domain is shaded. (**B**) Analysis of in vitro–translated ARP-1 and its mutants in a 15% SDS-polyacrylamide gel. Values in kilodaltons of ^{14}C-labeled protein markers (Amersham) are indicated. (**C**) Gel retardation of ARP-1 (lane 1) and its mutants translated in vitro (lanes 2 to 8, ΔA1 to ΔA7, respectively), cotranslated (lane 9, ARP-1 + ΔA1; lane 11, ARP-1 + ΔA2; lane 12, ARP-1 + ΔA6; lane 13, ΔA6 + ΔA7), or synthesized separately and then mixed (lane 10, ARP-1 + ΔA1) with the −222- to −146-fragment of the apoAI enhancer as the probe. (**D**) Gel retardation with oligo A probe (2.5 fmol) and different amounts of ARP-1 produced in COS-1 (lanes 1 to 5), or ΔA6 produced in COS-1 (lanes 6 to 10). Lanes 1 and 6, 0.06 μg; lanes 2 and 7, 0.3 μg; lanes 3 and 8, 1.5 μg; lanes 4 and 9, 3.0 μg; lanes 5 and 10, 10.0 μg (*21*). Complexes I, II, and III are denoted by arrows. (**E** and **F**) Titrations of retardation complex formation. Gel slices containing complexes I, II, and III and free probe were excised, counted in a scintillation counter, and plotted as percent of DNA bound in each complex.

REFERENCES AND NOTES

1. M. S. Brown and J. L. Goldstein, *Annu. Rev. Biochem.* **52**, 223 (1983).
2. J. L. Breslow, in *The Metabolic Basis of Inherited Disease*, C. R. Scriver *et al.*, Eds. (McGraw-Hill, New York, ed. 6, 1989), pp. 1251–1266.
3. I. A. Haddad, J. M. Ordovas, T. Fitzpatrick, S. K. Karathanasis, *J. Biol. Chem.* **261**, 13268 (1986); N. A. Elshourbagy *et al.*, *Proc. Natl. Acad. Sci. U.S.A.* **82**, 8242 (1985).
4. J. C. E. Miller *et al.*, *Proc. Natl. Acad. Sci. U.S.A.* **80**, 1511 (1983); M. Sorci-Thomas *et al.*, *J. Lipid Res.* **30**, 1397 (1989).
5. B. Staels *et al.*, *J. Lipid Res.* **30**, 1137 (1989).
6. T. K. Archer, S.-P. Tam, R. G. Deeley, *J. Biol. Chem.* **261**, 5067 (1986).
7. N. O. Davidson, R. C. Carlos, M. J. Drewek, T. G. Parmer, *J. Lipid Res.* **29**, 1511 (1988).
8. R. L. Widom, J. A. A. Ladias, S. Kouidou, S. K. Karathanasis, *Mol. Cell. Biol.* **11**, 677 (1991).
9. J. A. A. Ladias, M. Mietus-Snyder, Y. Yamashita, R. L. Widom, S. K. Karathanasis, unpublished results.
10. Phage λgt11 cDNA expression libraries were screened with oligo A probe, as described [C. R. Vinson, K. L. LaMarco, P. F. Johnson. W. H. Landschulz, S. L. McKnight, *Genes Dev.* **2**, 801 (1988)]. Oligo A was generated by annealing two oligomers, 5′-GATCACTGAACCCTTGACCCCT-

GCCCT-3′ and 5′-GATCAGGGCAGGGGTCAA-GGGTTCAGT-3′, and although it lacked the −222 to −215 region that is identical to Sp1 binding site, competed efficiently with site A for binding nuclear proteins. For library screening, oligo A was ^{32}P-labeled at the 5′ end with T4 polynucleotide kinase and self-ligated with T4 DNA ligase. Libraries were plated on *Escherichia coli* Y1090 and isopropylthiogalactoside (IPTG)-induced proteins were transferred to nitrocellulose filters. Filters were denatured in 6 M guanidine hydrochloride in binding buffer [20 mM Hepes, pH 7.9, 40 mM KCl, 3 mM $MgCl_2$, and 1 mM dithiothreitol (DTT)] at 4°C, followed by renaturation in a series of 5-min rinses in five successive 1:1 dilutions of the guanidine solution in binding buffer. After two final 5-min washes in binding buffer, filters were blocked for 30 min in binding buffer containing 5% nonfat dry milk (Carnation). Filters were incubated with probe (2×10^6 cpm/ml) in the presence of denatured, sonicated salmon sperm DNA (5 μg/ml) in binding buffer containing 0.25% nonfat dry milk at 4°C for 12 hours. Filters were washed in binding buffer with 0.25% milk and autoradiographed. Positive clones were purified and subjected to binding-specificity spot tests: ~10^6 plaque-purified phage were spotted on a preformed lawn of Y1090 *E. coli* and the plaques were tested for binding to various oligonucleotide probes as described above. To clone λHP-16, a human genomic DNA library was screened with the λHP-1 insert probe, and a clone containing ~800 bp of the 5′ λHP-1 sequence and extending ~15 kb to the 5′ direction was isolated; a nonrepetitive genomic fragment located upstream to sequences corresponding to λHP-1 was subsequently used as probe to screen the placenta cDNA library. The inserts from both λHP-1 and λHP-16 were subcloned in M13mp18 and sequenced [F. Sanger, S. Nicklen, A. R. Coulson, *Proc. Natl. Acad. Sci. U.S.A.* **74**, 5463 (1977); A. M. Maxam and W. Gilbert, *Methods Enzymol.* **65**, 499 (1980)]. Protein comparisons were carried out as described [D. Lipman and W. Pearson, *Science* **227**, 1435 (1985)].

11. N. Miyajima *et al.*, *Nucleic Acids Res.* **16**, 11057 (1988).
12. M. Mlodzik, Y. Hiromi, U. Weber, C. Goodman, G. Rubin, *Cell* **60**, 211 (1990).
13. A DNA fragment corresponding to ARP-1 DNA binding domain was used as probe to screen cDNA libraries from human placenta, liver, and HepG2 cells. Five different groups of clones were obtained and were termed ARP-1, ARP-2, ARP-3, ARP-4, and ARP-5. Sequence analysis identified ARP-2 as the Ear-3 (*11*), ARP-3 as the Ear-2 (*11*), and ARP-4 as the retinoic acid X receptor hRXRα [D. J. Mangelsdorf, E. S. Ong, J. A. Dyck, R. M. Evans, *Nature* **345**, 224 (1990)]. ARP-5 has not yet been characterized.
14. L.-H. Wang *et al.*, *Nature* **340**, 163 (1989).
15. R. M. Evans, *Science* **240**, 889 (1988); S. Green and P. Chambon, *Trends Genet.* **4**, 309 (1988); M. Beato, *Cell* **56**, 335 (1989).
16. C. K. Glass, J. M. Holloway, O. V. Devary, M. G. Rosenfeld, *Cell* **54**, 313 (1988).
17. V. Kumar and P. Chambon, *ibid.* **55**, 145 (1988); S. Y. Tsai *et al.*, *ibid.*, p. 361.
18. S. E. Fawell, J. A. Lees, R. White, M. G. Parker, *ibid.* **60**, 953 (1990).
19. P. J. Godowski, S. Rusconi, M. Miesfeld, K. R. Yamamoto, *Nature* **325**, 365 (1987); F. C. Dalman *et al.*, *J. Biol. Chem.* **264**, 19815 (1989).
20. K. N. Sastry, U. Seedorf, S. K. Karathanasis, *Mol. Cell. Biol.* **8**, 605 (1988).
21. The Eco RI insert of λHP-1 was cloned in the expression vector pMT2 [R. J. Kaufman, M. V. Davies, V. K. Pathak, J. W. Hershey, *Mol. Cell. Biol.* **9**, 946 (1989)], in both sense (construct pMA) and antisense (construct pMB) orientations. The construct pMA6, which contains the 1–170 ARP-1 region cloned in pMT2, was made by digestion of pGEM–ARP-1A with Bam HI, religation of the fragment that contained the vector but lacked the ARP-1 COOH-terminus, digestion with Hinc II (site in the vector), and ligation in the presence of an oligo (5′-GGTGAGTGAGTGAGAATTCTCACT-CACTCACC-3′), that contained an Eco RI site and termination codons in all frames. The resulting clone was used to prepare an Eco RI fragment that contained the 1–170 ARP-1 region, which was cloned in pMT2. The pMA, pMB, and pMA6 constructs were transfected in COS-1 cells, and whole-cell extracts were prepared by three cycles of freezing-thawing in buffer 2× buffer A. The deletion mutants ΔA2, ΔA3, ΔA4, ΔA5, and ΔA6 were generated by digestion of pGEM–ARP-1A with Hind III, Hinc II, Pst I, Sph I or Bam HI, respectively. The 3′ overhangs generated by Pst I and Sph I were converted to blunt ends with Klenow DNA polymerase before in vitro transcription. The mutant ΔA1 was generated by polymerase chain reaction (PCR) [R. K. Saiki *et al.*, *Science* **239**, 487 (1988)] with the primer 5′-GATGAATTCGCCGCCAC-CATGGAGTGCGTGGTGTGCGGAGA-3′, which provides a Kozak sequence [M. Kozak, *J. Cell Biol.* **108**, 229 (1989)] and an initiation codon, the M13 universal primer, and the ARP-1 cDNA cloned into M13 as a template. The PCR product was cloned in pGEM-4 (SP6 promoter), and confirmed by sequencing. Digestion of this clone with Bam HI generated ΔA7.
22. K. Gorski, M. Carneiro, U. Schibler, *Cell* **47**, 767 (1986).
23. G. Shaw and R. Kamen, *ibid.* **46**, 659 (1986).
24. J. Sambrook, E. Fritsch, T. Maniatis, *Molecular Cloning* (Cold Spring Harbor Laboratory, Cold Spring Harbor, NY, 1989).
25. K. Reue, T. Leff, J. L. Breslow, *J. Biol. Chem.* **263**, 6857 (1988).
26. H. K. Das, T. Leff, J. L. Breslow, *ibid.*, p. 11452.
27. Y.-P. Hwung *et al.*, *Mol. Cell. Biol.* **8**, 2070 (1988).
28. L. Klein-Hitpass *et al.*, *ibid.* **9**, 43 (1989).
29. P. Monaci, A. Nicosia, R. Cortese, *EMBO J.* **7**, 2075 (1988).
30. R. H. Costa, D. R. Grayson, J. E. Darnell, *Mol. Cell. Biol.* **9**, 1415 (1989).

31. We thank T. Hai for the human placenta library; R. Kaufman and L. Zon for the pMT2 vector; H. Winter for fetal human tissue samples; A. Andreadis, R. Breitbart, J. Rottman, and C. Smith for critical reading of the manuscript; and E. McIntosh for the artwork. S.K.K. is an Established Investigator of the American Heart Association (AHA). This work was supported by grants from NIH and AHA.

9 July 1990; accepted 12 November 1990

Cortical Computational Maps Control Auditory Perception

HIROSHI RIQUIMAROUX,* STEPHEN J. GAIONI,* NOBUO SUGA†

Mustached bats orient and find insects by emitting ultrasonic pulses and analyzing the returning echoes. Neurons in the Doppler-shifted constant-frequency (DSCF) and frequency-modulated (FM-FM) areas of the auditory cortex form maps of echo frequency (target velocity) and echo delay (target range), respectively. Bats were trained to discriminate changes in echo frequency or delay, and then these areas were selectively inactivated with muscimol. Inactivation of the DSCF area disrupted frequency but not delay discriminations; inactivation of the FM-FM area disrupted delay but not frequency discriminations. Thus, focal inactivation of specific cortical maps produces specific disruptions in the perception of biosonar signals.

THE JAMAICAN MUSTACHED BAT (*Pteronotus parnellii parnellii*) uses biosonar pulses to orient and to hunt flying insects. Its auditory cortex (AC) is specialized for processing information contained in the pulse (P) and its echo (E). The AC has at least ten functional areas (Fig. 1A), each containing one or more maps that represent a P-E parameter or combination of parameters important for encoding a particular type or types of biosonar information (*1*).

The P of the mustached bat has four harmonics (H_{1-4}), each consisting of a long constant-frequency (CF_{1-4}) component followed by a short frequency-modulated (FM_{1-4}) component (Fig. 1B). Of these, H_2 is always the most intense. When a bat is not flying, its PCF_2 is about 61.0 kHz (*2*, *3*).

During insect pursuit, the mustached bat adjusts its P frequency to stabilize the CF_2 of Doppler-shifted echoes at a reference frequency ~200 Hz above its resting frequency (*4*, *5*). This behavior is known as Doppler shift (DS) compensation. Because the peripheral auditory system of the mustached bat has a disproportionately large number of neurons that are sharply tuned around the reference frequency, the CF_2 of DS-compensated echoes is subjected to fine frequency analysis (*6*). The accuracy of the bat's DS compensation depends on its ability to resolve the frequency of the Doppler-shifted ECF_2.

The cortical area most likely to play a major role in the fine frequency analysis of Doppler-shifted echoes is the Doppler-shifted CF (DSCF) processing area of the primary AC (*7*, *8*). This area is tonotopically organized but only represents frequencies in the range of ECF_2 from 60.6 to 62.3 kHz (*2*). The frequency tuning curves of DSCF neurons are very narrow, even at high stimulus intensities (*8*). Further, bats with bilateral ablation of the DSCF may not be able to detect small echo DSs (*4*).

To determine the range of a target, the mustached bat measures the delay between the emitted P and the returning E. The FM-FM area of the AC probably plays a

Department of Biology, Washington University, St. Louis, MO 63130.

*The first two authors contributed equally to the report.
†To whom correspondence should be addressed.